Selective Catalytic Oxidation of Ammonia to Nitrogen on CuO-CeO_2 Bimetallic Oxide Catalysts

Chang-Mao Hung*

Department of Business Administration, Yung-Ta Institute of Technology & Commerce, 316 Chung-shan Road, Linlo, Pingtung 909, Taiwan, R.O.C.

Abstract

This study addresses the performance of the selective catalytic oxidation (SCO) of ammonia to N_2 over a CuO-CeO_2 bimetallic oxide catalyst in a tubular fixed-bed reactor (TFBR) at temperatures from 423 to 673 K in the presence of oxygen. CuO-CeO_2 bimetallic oxide catalyst was prepared by co-precipitation with $Cu(NO_3)_2$ and $Ce(NO_3)_3$ at various molar concentrations. This study tested operational stability and investigated how the influent NH_3 concentration (C_0 = 500-1000 ppm) influences the capacity to remove NH_3. The catalysts were characterized using XRD, FTIR, PSA, SEM and EDX. Ammonia was removed by oxidation in the absence of CuO-CeO_2 bimetallic oxide catalyst, and the formation of copper (II) and cerium (IV) oxide active sites was confirmed. Additionally, the effects of the NH_3 content of the carrier gas on the catalyst's reaction rate (r) were observed. The results revealed that the extent of catalytic oxidation of ammonia in the presence of a CuO-CeO_2 bimetallic oxide catalyst was a function of the molar ratio Cu:Ce in the bimetallic catalyst. The kinetics of catalyzed NH_3 oxidation are described using the rate expression of the Eley-Rideal kinetic model. Also, experimental results indicate a reasonable mechanism for the catalytic oxidation of ammonia.

Keywords: Catalytic Selective Oxidation (SCO), Tubular Fixed-bed Reactor (TFBR), Ammonia, Co-precipitation, CuO-CeO_2 Bimetallic Oxide Catalyst.

* Corresponding author. Tel: 886-8-723-3733; Fax: 886-8-721-0090

E-*mail address*: cmhung@mail.ytit.edu.tw

INTRODUCTION

Extensively adopted into industrial processes, ammonia (NH_3) can be eliminated in numerous ways. NH_3 is used in the ammonium nitrate and nitric acid production industry, livestock feedlots, urea manufacturing plants, the nitrogen fertilizer application industry, fossil-fuel combustion and petroleum refineries, as well as the refrigeration industry. Ammonia is a toxic inorganic gas with a pungent odor under ambient conditions, and is potentially harmful to public health (Mojtahedi and Abbasian, 1995; Giroux et al., 1997; Kurvits and Matra, 1998; Amblard et al., 2000; Hung et al., 2003; Sotiropoulou et al., 2004). Conventional biological, physical and chemical treatments, including biofilters (Kim et al., 2000; Chung et al., 2001), stripping (Huang et al., 2000), scrubbing with water (Burch and Southward, 2001), post-combustion control (Hasegawa and Sato, 1998), microwave-plasma discharge (Wójtowicz et al., 2000), electrochemical oxidation (de Vooys et al., 2001) and the use of activated carbon fibers (ACFs) for soot adsorption (Mangun et al., 1999; Muenter and Koehler, 2000), only trigger a phase transformation and may yield a contaminated sludge and/or an adsorbent, both of which require further treatment. The maintenance and operating costs associated with these physical and/or chemical methods are high. Therefore, the removal and the control and prevention, of the emission of ammonia emission from air and waste streams are important. Discharges present challenges because environmental laws and regulations on safe discharge are becoming increasingly strict.

More recently, catalytic oxidation has been established to increase the effectiveness of AOP (Advanced Oxidation Processes) technology using dedicated catalysts, which potentially shorten the reaction times of oxidation, and allow it to proceed under milder operating conditions. The selective catalytic oxidation (SCO) of ammonia in a stream to molecular nitrogen and water is one method for solving problems of ammonia pollution (Wöllner et al., 1993; Schmidt-Szałowski et al., 1998; Wang et al., 1999; Curtin et al., 2000; Lietti et al., 2000; Amblard et al., 2000; Escandón et al., 2002; Dravell et al., 2003). The catalytic oxidation of ammonia has been reported to proceed as follows;

$$4NH_3 + 3O_2 \rightarrow 2N_2 + 6H_2O \quad (1)$$

$$2NH_3 + 2O_2 \rightarrow N_2O + 3H_2O \quad (2)$$

$$4NH_3 + 5O_2 \rightarrow 4NO + 6H_2O \quad (3)$$

The SCO process that involves ammonia should be selective for nitrogen (reaction 1) and prevent further oxidation of nitrogen (reactions 2 and 3). Earlier work on ammonia oxidation was reviewed by Il'chenko (1975a, 1975b, 1976), who focused on the reaction mechanism of ammonia oxidation, and compared catalytic activities. Few catalysts have been used in oxidizing ammonia in the gaseous phase. For instance, Amblard et al. (2000) demonstrated excellent selective conversion of ammonia to nitrogen (> 90%) by γ-Al_2O_3-supported Ni by selective catalytic oxidation. Moreover, Wang et al. (1999), who developed Ni-based catalysts for oxidizing fuel gas generated by gasifying biomass, found that fresh Ni-based catalysts were more active at lower temperatures in decomposing ammonia, and the partial pressure of hydrogen in the flue gas is a critical factor that governed ammonia oxidation. Liang (2000) studied the oxidation of ammonia in a fixed-bed microreactor in the temperature range 873-1023 K at GHSV=1800-3600 hr^{-1}. They found that the conversion of ammonia reached 98.7% and 99.8% on nitrided MoNx/α-Al_2O_3 and NiMoNy/α-Al_2O_3 catalysts, respectively. Schmidt-Szałowski (1998) also developed a hypothetical model of the effect of these catalysts and their activity and selectivity in oxidizing ammonia.

Lou and Chen (1995a) employed a catalyst that comprised a foam Pt, Ni and Cr alloy to elucidate the kinetics of the catalytic incineration of butanone and toluene. He determined that the Mars and van Krevelen model was suitable for describing the catalytic incineration of the VOCs. Lou and Lee (1997) used a Pt/Al_2O_3 alloy catalyst to clarify the kinetics of the catalytic incineration of trichloromethane. He applied power-rate law kinetics and found that the reaction was first-order in the trichloromethane concentration and that the activation energy was 16.2 kcal/mol. Lou and Lee (1995b) also utilized a 0.05% Pt/Ni/Cr alloy catalyst to investigate the kinetics of the catalytic incineration of trichloromethane. According to their results, the Mars and van Krevelen Model was appropriate for describing the catalytic incineration of these VOCs. Gangwal (1988) used a 0.1% Pt, 3% Ni/ γ-Al_2O_3 catalyst to elucidate the kinetics of deep catalytic oxidation with n-hexane and benzene. According to their results, the Mars and van Krevelen model was favorable for explaining the catalytic combustion of a binary mixture, at temperatures between 433 and 633 K. Recently, Auer and Thyrion (2002) employed an integral fixed-bed reactor over an $La_{0.9}Ce_{0.1}CoO_3$ perovskite catalyst to examine the kinetics of total oxidation with methane. They favored the SED (Sequential Experimental Design) model to explain the catalytic combustion of water in feed, at temperatures from 633 to 773 K. Spivey (1987) excellently reviewed recent work on the modeling of the catalytic oxidation of VOCs. Nitrogen compounds have been similarly examined and have been demonstrated reversibly to inhibit the catalyst (Richardson, 1989). However, the kinetics of the catalytic oxidation of NH_3 on metal composite catalysts have not been comprehensively examined.

Copper oxide is a highly active transition metal, and has been considered to be a potential substitute for noble metal-based emission control catalysts (Gang et al., 1999). Copper oxide on

cerium oxide is known to constitute an efficient catalyst for various reactions, such as the combustion of CO and the water-gas-shift (WGS) reaction (Sedmak et al., 2004; Fu et al., 2003). Furthermore, the most important washcoat component of a catalyst is cerium, which is added to the washcoat as a stabilizer and an oxygen-storage component. Cerium stabilizes the washcoat layer improves the thermal resistance enhances the catalytic activity of precious metals, and provides oxygen storage/release capacity (OSC) (Golunski et al., 1995; Petryk and Kolakowska, 2000; Wey et al., 2002; González-Velasco et al., 2003). The interaction between copper oxide and the cerium is complex, because various copper-cerium interactions can result in synergistic effects, enhancing catalytic characteristics (Skårman et al., 2002). However, little work has been performed on the use of $CuO\text{-}CeO_2$ bimetallic oxide catalyst to evaluate the reactive characteristics of these active metals in selective catalytic oxidation. Therefore, given the low cost of copper, this study considers the effect of the $CuO\text{-}CeO_2$ bimetallic oxide catalyst system on the oxidation of ammonia-containing gas streams with various parameters, and the kinetics of the removal of ammonia from the gas-phase in an SCO process. X-ray powder diffraction (XRD), Fourier transform infrared spectroscopy (FTIR), SEM, energy-dispersive X-ray spectrometry (EDX) and a particle size analyzer (PSA), were all employed to characterize the $CuO\text{-}CeO_2$ bimetallic oxide catalyst.

MATERIALS AND METHODS

Preparing $CuO\text{-}CeO_2$ Bimetallic Oxide Catalyst

$CuO\text{-}CeO_2$ bimetallic oxide catalysts were prepared by co-precipitating copper (II) nitrate (GR grade, Merck, Darmstadt, Germany) with cerium (III) nitrate (GR grade, Merck, Darmstadt, Germany) using K_2CO_3 (0.2 M) at four molar ratios: 6:4, 7:3, 8:2 and 9:1. The pH of the co-precipitating aqueous solution was 11.5 ± 0.2. After filtration, the co-precipitating aqueous solution was washed five times with deionized water, and dried at 393 K. These compounds were then calcined at 773 K in an air stream for 4 hours. The powder thus produced was formed into tablets using acetic acid as a binder. The tablets were later reheated at 573 K to burn the binder out of the $CuO\text{-}CeO_2$ bimetallic oxide catalyst. They were then crushed and sieved into particles of various sizes from 0.15 and 0.25 mm, for later use.

Characterizing the Solid Phase

X-ray diffractograms were obtained using a Diano-8536 diffractometer with CuKα radiation as the source. During analysis, the sample was scanned from 20 to 80° at a rate of 0.4°/min. Diffuse reflectance FTIR spectra of species adsorbed on the catalyst were measured at room temperature using a Bruker Vector 22 FTIR spectrometer, equipped with a diffuse reflectance attachment with a resolution of 4 cm^{-1} (Bruker, Germany). The changes in the sizes of the catalytic particles were

measured using a laser light-scattering particle size analyzer (PSA, Coulter LS100, USA). Scanning electron microscopy, using an energy-dispersive X-ray spectrometer (SEM/EDX, JEOL, JSM-6400, Kevex, DeltaII), yielded the morphology of the catalysts and provided information on the distribution of copper and cerium on the surfaces of the catalysts.

Reaction System

Experiments were conducted on a tubular fixed-bed flow quartz reactor (TFBR). Two flowing gases, NH_3 and O_2, were used to prepare the feed mixture in the diluting gas, helium, which flowed into the inlet of the reactor. A mass flow regulator was used to control independently the flows of ammonia and oxygen. Extremely pure helium was used as a carrier gas at a flow rate from 8 to 13 L/min, controlled using a mass flow meter (830 Series Side-Trak^{TM}, Sierra, Monterey, CA, USA). The mass of each catalyst was 1 g and the empty bed volume was approximately 1.2 cm^3. An inert material formed from (hydrophilic and inert) γ-Al_2O_3 spheres was used to increase the interfacial area between the solid and the gas phase to increase the mass transfer of ammonia from gaseous streams. This approach resembled that of Huang (2000), who conducted experiments on the catalytic oxidation of ammonia. A reaction tube with a length of 300 mm and an inner diameter of 28 mm was placed inside a split tube furnace. The tube that contained the catalyst was placed in the same furnace. The temperature was measured using two type-K thermocouples (KT-110, Kirter, Kaohsiung, Taiwan), each with a diameter of 0.5 mm, these were located in front of and behind the catalytic bed. The thermocouples were also connected to a PID controller (FP21, Shimaaen, Tokyo, Japan) to maintain the temperature in the tube within ±0.5%. The concentration of the feed gas (GHSV, 92,000 ml/h-g) was maintained at 1,000 ppm NH_3 and the O_2 concentration was 4%. The catalyst was not deactivated during testing. Fig. 1 schematically depicts the tubular fixed-bed reaction system (TFBR).

Analyses

Before and after the reaction, samples were automatically injected through a sampling valve into a gas chromatograph (Shimadzu GC-14A), equipped with a thermal conductivity detector. A stainless-steel column (Porapak Q 80/100mesh) was used to separate and determine the concentrations of N_2O isothermally at 100 ℃. The areas associated with the signals were electronically measured using a data integrator (CR-6A, Shimadzu, Kyoto, Japan). Dilute sulfuric acid was used to scrub the residual ammonia in the vapor gas and the amount present was measured using a Merck kit (Merck, Spectroquant Vega 400, Darmstadt, Germany). The concentrations of NO, NO_2,, and O_2 in the gas samples were monitored continuously during combustion at a particular location, using a portable flue gas analyzer (IMR-3000, Neckarsulm, Germany). Data were collected when the SCO reaction was in a steady state, typically after 20 min at each temperature. Each temperature was maintained for 90 min to allow the system to

enter a steady state. Most experiments were repeated once to ensure reproducibility, and similar results were always obtained.

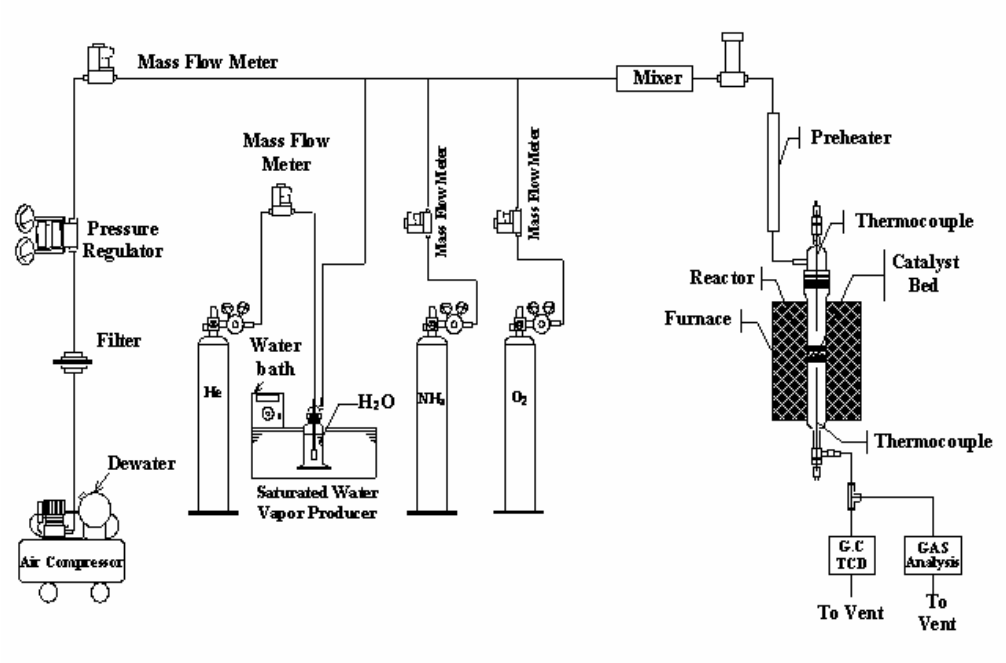

Fig. 1. Schematic diagram of the tubular fixed-bed reaction (TFBR) system.

RESULTS AND DISCUSSION

Characterizing CuO-CeO_2 Bimetallic Oxide Catalyst

Fig. 2 presents the X-ray diffraction (XRD) patterns obtained at various copper-cerium molar ratios, verifying that CuO and CeO_2 are the dominant phases of the copper-cerium composite catalyst. Dominant CuO diffraction peaks were observed at around 2θ=35.5, 38.8, 48.7, 53.4, 61.4, 66.3 and 68.0^o when a copper-cerium composite catalyst was used. This result is similar to that obtained by Ning (2001). Moreover, CeO_2 diffraction peaks were present at approximately 2θ=28.5, 33.1, 47.5 and 56.7^o when a copper-cerium composite catalyst was used. This result is similar to that reported by Hashimoto (2000). An earlier investigation demonstrated that CeO_2 is the most active phase in a catalytic reaction, because it has been demonstrated to be a strong promoter of an oxygen-storage medium, whenever noble metals are used as major catalysts (Golunski et al., 1995; Petryk and Kolakowska, 2000). Cerium dioxide in a copper catalyst can be assumed to promote the formation of the active phase of CuO under the conditions of ammonia oxidation. Additionally, CeO_2-based materials can act as oxygen buffers by storing/releasing O_2, because the automotive three-way catalytic converter contains the cerium (III)-cerium (IV) redox couple (Kašpar et al., 1999). Thus, X-ray powder diffraction confirmed the formation of copper

(II) and cerium (IV) oxide active sites, synergistically affecting the Cu/Ce cooperation in the redox mechanism.

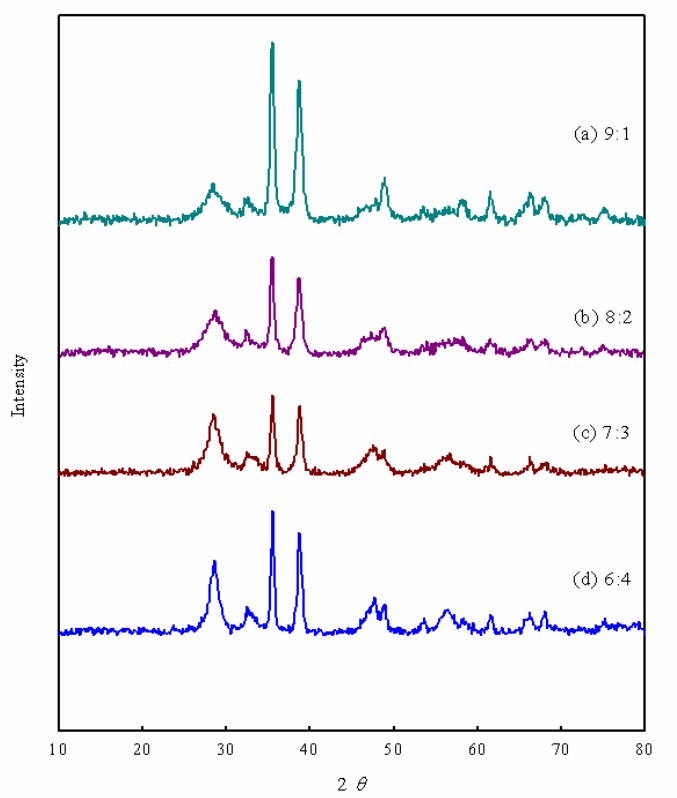

Fig. 2. XRD pattern of the various metal content on the CuO-CeO_2 bimetallic oxide catalyst for the conversion of NH_3.

Fig. 3 compares the FTIR spectra at various copper-cerium molar ratios, and also confirms the presence of the CuO-like phase and the CeO_2 phase on the surface of the copper-cerium composite catalyst. Fig. 3 reveals that the peaks associated with the CuO-like phase on the framework are associated with a peak at around 1,384 cm^{-1} (Sadykov et al., 2001; Hadjiivanov, 2000). Fig. 3 also shows that the CeO_2 phase on the framework is associated with peaks at around 1,630 cm^{-1}, 1,524 cm^{-1} and 1,380 cm^{-1} (Centi and Perathoner, 1998). CuO and CeO_2 are normally accepted to exhibit great synergy effect when they are both prepared as a composite CuO/CeO_2 catalyst (Sedmak et al., 2004). Therefore, we suggest here that the catalytic activity of the CuO-CeO_2 bimetallic oxide catalyst system in oxidizing ammonia may be explained by the reversible redox behavior of CuO/CeO_2 couples in promoting the bifunctional mechanism.

The change in the sizes of particles of the catalyst was determined using the laser light-scattering method, as depicted in Fig. 4. The mean particle size converged to approximately 14.3, 14.6, 10.3, and 7.7 μm, for fresh copper-cerium composite catalysts with the four molar ratios:

6:4, 7:3, 8:2 and 9:1. However, the diameters of the catalyst decreased as the copper content declined, indicating that co-precipitation aggregates the low metal molar ratio.

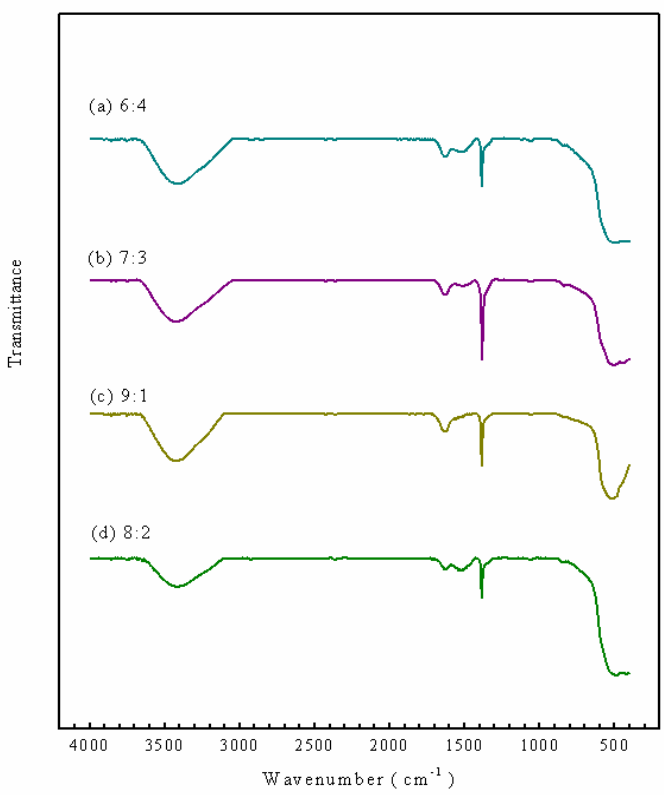

Fig. 3. FTIR pattern of the various metal content on the CuO-CeO_2 bimetallic oxide catalyst for the conversion of NH_3.

Oxidizing Ammonia

Catalysts with various copper and cerium contents were prepared, characterized and tested for their effectiveness in the SCO process. Fig. 5 plots the effects of composite catalysts with various copper-cerium molar ratios on the extents of conversion of NH_3, in terms of the extent of removal during SCO. The copper-cerium molar ratio of the copper-cerium composite catalyst governs the extent of catalytic oxidation of NH_3 over it. The extents of conversion of NH_3 were 99.0% and 92.0% when the catalytic oxidation proceeded under particular operating conditions over copper-cerium composite catalysts with molar ratios of 6:4 and 9:1, respectively. Notably, a higher cerium content was associated with a higher NH_3 conversion. The overall maximum selectivity of N_2 production varied from 27% to 86%, and that of NO production varied from 0% to 13% over the range 23-99% NH_3 conversion at NH_3 concentrations of 1,000 ppm over the copper-cerium (6:4) composite catalyst (Table 1). The only intermediate species was NO. The decrease in the nitrogen selectivity is primarily related to the formation of NO. This result is consistent with the findings of Gang (1999). Nitrogen gas is believed to be generated mostly by the dissociation of

NO produced by the oxidation of adsorbed NH_3 (Bradely et al., 1995). Accordingly, this work considers the hypothesis that NH_3 and oxygen may be adsorbed to specific sites on the copper-cerium (6:4) composite catalyst, accelerating the conversion of NH_3 to nitrogen. Based on these results, nitrogen was the dominant gas and a small amount of NO was detected in the resultant stream. This result is similar to those of Li (1997) and Curtin (2000).

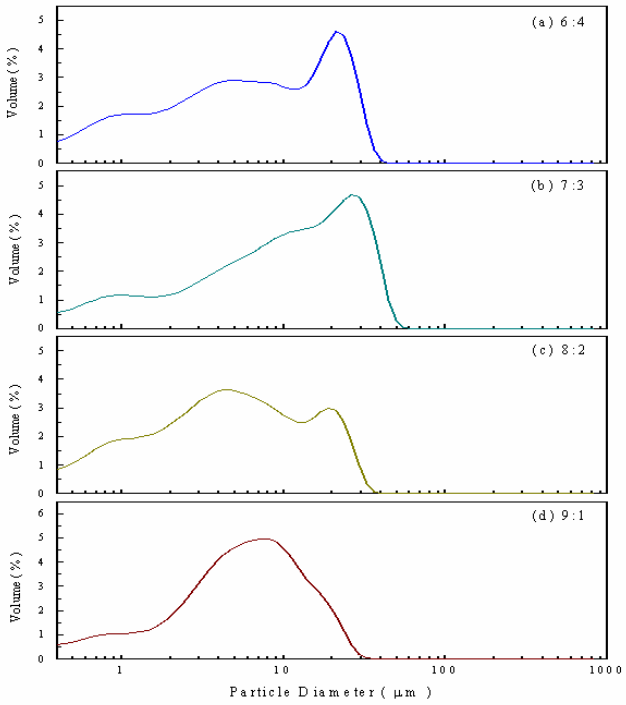

Fig. 4. Changes in particle sizes distribution of the various metal content on the CuO-CeO_2 bimetallic oxide catalyst for the conversion of NH_3.

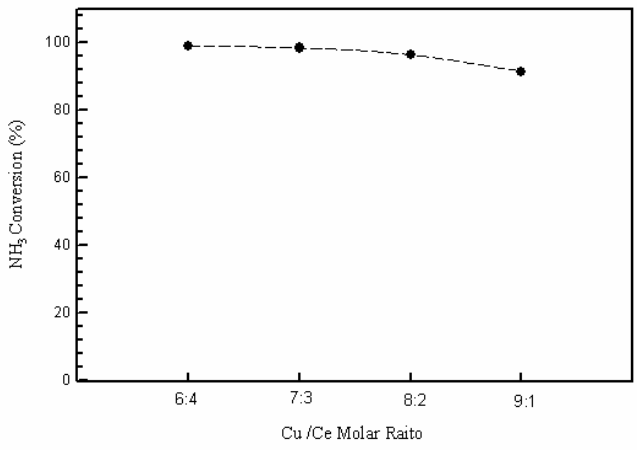

Fig. 5. Effect of the metal content on the CuO-CeO_2 bimetallic oxide catalyst for the conversion of NH_3. Test conditions: 1,000 ppm NH_3 in He, O_2=4%, temperature= 673 K, R.H.=12%, GHSV=92,000 ml/h-g.

Table 1. Product selectivity from ammonia oxidation using $CuO\text{-}CeO_2$ bimetallic oxide catalyst of the various metal content (Test conditions: 1,000 ppm NH_3 in He, O_2=4%, temperature=423-673 K, R.H.=12%, GHSV＝92,000 ml/h-g).

Molar ratio	Ammonia conversion(%)	Product selectivity (%)			
		N_2	NO	NO_2	N_2O
6:4	23–99	27–86	0–13	N.D.	N.D.
7:3	12–98	12–73	0–24	N.D.	N.D.
8:2	14–96	13–78	0–18	N.D.	N.D.
9:1	13–92	13–70	0–21	N.D.	N.D.

Figs. 6 and 7 depict the surface morphological changes of copper-cerium (6:4) composite catalyst, identified by scanning electron microscopy (SEM) with elemental dot mapping photographs, for copper-cerium with various metal contents. These figures thus provide information on the surface structures of fresh and aged catalysts. The observations of agglomerates by SEM reveal that the composite catalyst particles are shaped into fine sheet-rod-like. Moreover, Fig. 6 shows a catalyst whose surface is more aggregated and crystalline than that in Fig. 7.

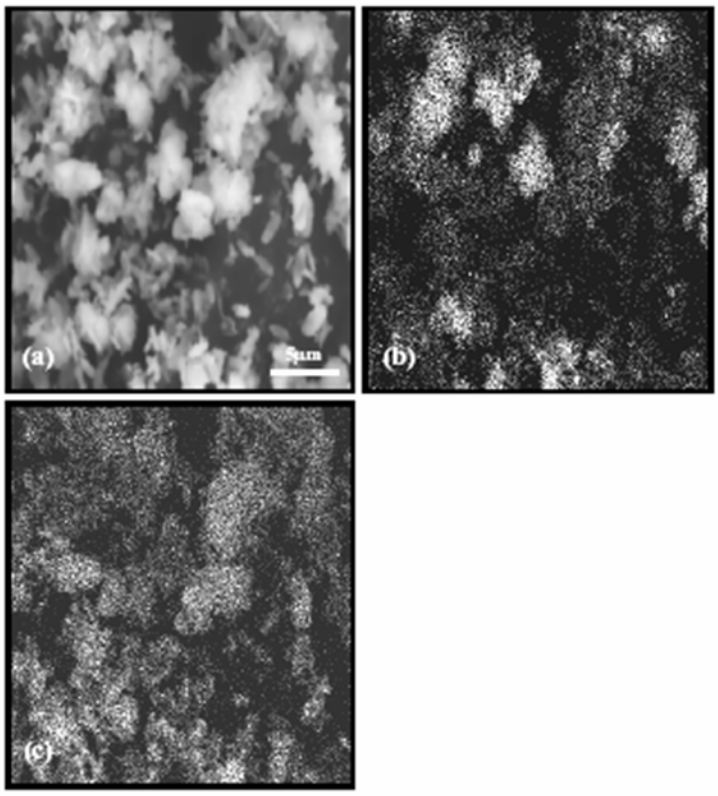

Fig. 6. SEM with dot mapping photographs result of various contents on the fresh $CuO\text{-}CeO_2$ (6:4) bimetallic oxide catalyst. (a) Original magnification: × 3,000, (b) Cu and (c) Ce.

Fig. 7 indicates that disaggregated and dispersed phases were formed when the surface of the catalyst was aged or when poisoning was caused by plugging, indicating that the porosity of the particles had changed. These crystal phases may be responsible for the high activity of the catalysts. The findings also confirm that the dispersion phenomena of the catalyst increased the efficiency of the removal of NH_3. The elemental distribution proportional to these particles was homogeneous, as shown by the electron backscattering in SEM micrographs (Figs. 6 and 7). Furthermore, elemental dot mapping photographs reveal that, after the elemental composition of the surfaces of the test catalysts had been activated, the metal content of the copper-cerium composite catalyst was slightly changed. Copper was present at an elemental percentage of 62% to 58% and cerium was present at an elemental percentage of 41% to 36% of the catalyst.

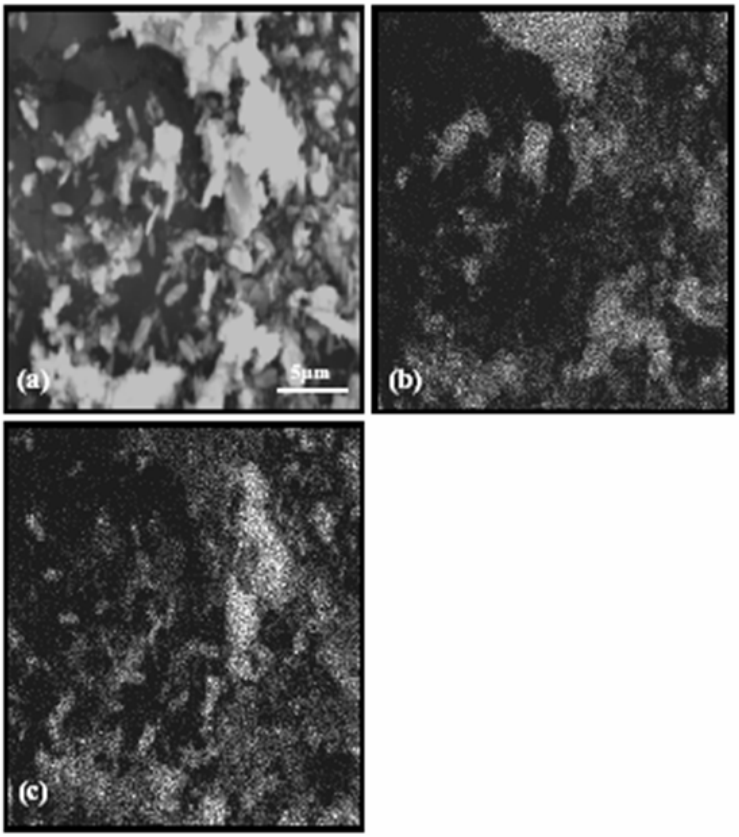

Fig. 7. SEM with dot mapping photographs result of various contents on the fresh CuO-CeO_2 (6:4) bimetallic oxide catalyst after activity test. (a) Original magnification: × 3,000, (b) Cu and (c) Ce. Test conditions : 1,000 ppm NH_3 in He, O_2=4%, R.H.=12%, GHSV=92,000 ml/h-g.

Reaction Kinetics

The effect of the NH_3 content of the carrier gas on the reaction rates (r) associated with the copper-cerium composite catalyst was considered. The reaction rate (r) of NH_3 is defined as follows.

$$-r = \frac{v}{V}(C_{i0} - C_i) = \frac{F}{V}(X_i - X_{i0}) \tag{4}$$

where v represents the volume flow rate (ml/s) of NH_3; V is the reaction volume (ml), and C_{i0} and C_i are the concentrations of NH_3 at the inlet and the outlet, respectively. The ratio F/V specifies the space velocity. X_i and X_{i0} represent the conversion of NH_3 at the inlet and the outlet, respectively. Fig. 8 presents the effects of NH_3 concentration and reaction temperature on the reaction rate over the CuO-CeO_2 (6:4) bimetallic oxide catalyst. The reaction rate (r) increases almost linearly with the NH_3 content at various temperatures. The reaction rates also increases with temperature above 423 K. The results also reveal that the CuO-CeO_2 (6:4) bimetallic oxide catalyst is very active in ammonia decomposition. Therefore, the extent removal of ammonia increased markedly with the temperature of the influent stream because the retention time during the catalytic process is reduced. The catalytic effect on the reduction of ammonia reduction was insignificant in the influent stream with ammonia concentrations from 500 to 1,000 ppm. Increasing the ammonia concentration to 500 ppm dramatically reduced the extent of the removal of ammonia.

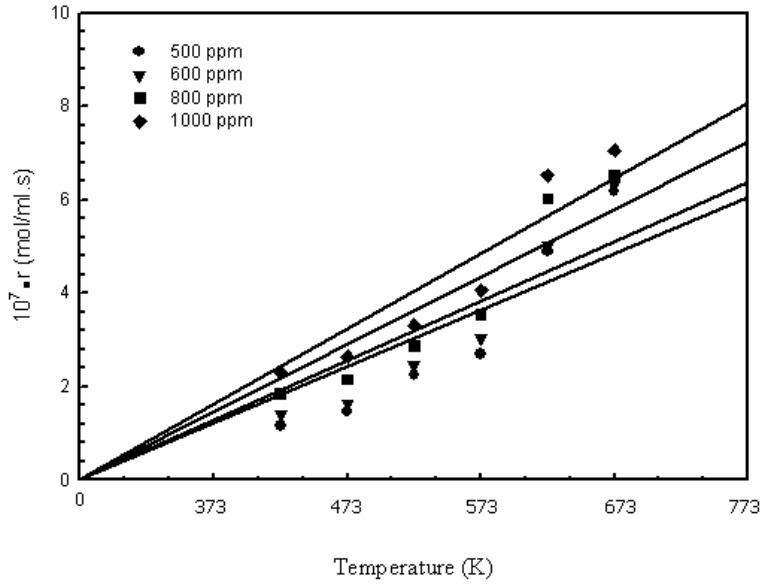

Fig. 8. Effect of various ammonia concentrations and different temperatures with reaction rates on the CuO-CeO_2 (6:4) bimetallic oxide catalyst for the conversion of NH_3. Test conditions: 500-1,000 ppm NH_3 in He, O_2=4%, R.H.=12%, GHSV=92,000 ml/h-g.

Fig. 9 plots *ln (1-X)* versus time at various reaction temperatures, using a CuO-CeO_2 (6:4) bimetallic oxide catalyst. A higher space time resulted in lower catalytic efficiency at a particular temperature. The plot is of a linear relationship between *ln (1-X)* and space time, and supports the

fact that the reaction is of first order. Previous studies by Huang (2000) and Long (2001) have found a first order dependency of the rate on NH_3 concentration. The reaction rate constants obtained from various kinetic models normally vary with temperature. The Arrhenius Equation can be determined using a typical method for calculating the activation energy of the reaction, where t is defined as follows.

$$k = A\exp\left(-Ea/RT\right) \tag{5}$$

where A is the frequency factor (sec^{-1}); Ea is the activation energy (kcal/mol); R is the ideal gas constant, and T represents the absolute temperature (K). Therefore, the reaction order can be determined from the slopes of the lines in Fig. 9. The linearity of the plots reveals that the kinetics are approximately first-order of the NH_3 oxidation varies from 0.55 to 0.94. Moreover, the reaction constant k is determined from the intercept of each line. Also, the plot *ln (1-X)* versus space time in Fig. 10 is a straight line. The intercept and gradient and the Arrhenius relationships give the pre-exponential factor [$A = 2.02\times10^8$ sec^{-1}] and the apparent activation energy of the oxidation of NH_3 (E_a = 14.8 kcal/mol). The model has been suggested to be appropriate for the oxidation of ammonia over CuO-CeO_2 bimetallic oxide catalyst, since the R^2 value (R^2 = 0.9285) for the fitting of the rate constants is relatively high.

The consistency of the results and first-order reaction kinetics supports the assertion that the catalytic reaction of NH_3 proceeds as follows.

$$O_2 + reduced\quad catalyst \xrightarrow{K_1} oxidized\quad catalyst \tag{6}$$

$$NH_3 + oxidized\quad catalyst \xrightarrow{K_2} reduced\quad catalyst + products \tag{7}$$

In this mechanism, the above steps are assumed to be first-order in the respective gaseous species. Reaction (6) describes the adsorption of oxygen molecules onto the surface active site of the catalyst.

The adsorbed oxygen molecule is decomposed and considered to be the active oxygen atom. In Eq. (7), the active oxygen atom reacts with the gaseous NH_3 molecule and yields the products. The reaction rates, r_1 and r_2, are defined as follows.

$$-r_1 = k_1 Co_2\left(1-\theta\right) \tag{8}$$

$$-r_2 = k_2 C_{NH_3}\theta \tag{9}$$

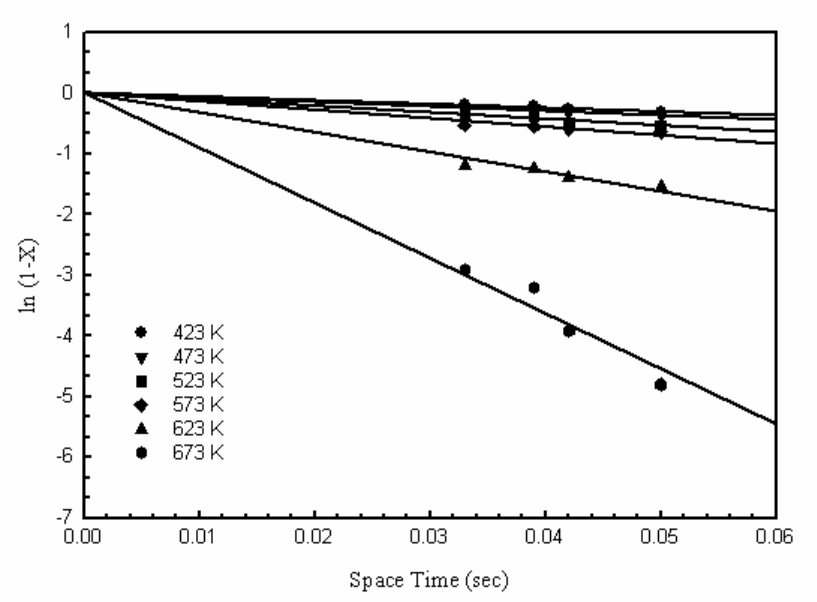

Fig. 9. Effect of the space time with the fractional conversion (X) on the CuO-CeO_2 (6:4) bimetallic oxide catalyst for the conversion of NH_3. Test conditions: 1,000 ppm NH_3 in He, O_2=4%, R.H.=12%, GHSV=92,000 ml/h-g.

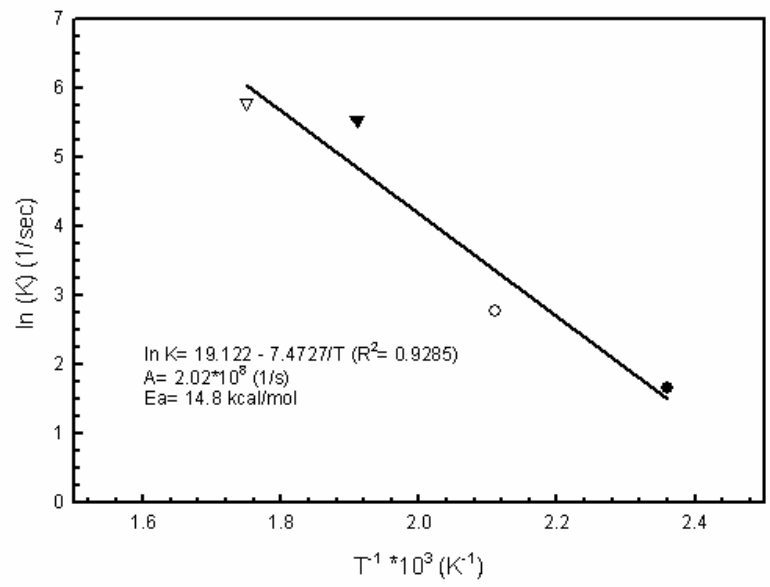

Fig. 10. Arrhenius plots of rate constants on the CuO-CeO_2 (6:4) bimetallic oxide catalyst for the conversion of NH_3.

in which k_1 and k_2 are the reaction rate constants of NH_3; C_{O_2} and C_{NH_3} are the concentrations of oxygen and NH_3, and θ is the proportion of the surface of the catalyst onto which O_2 is adsorbed. Therefore, a pseudo steady state condition is specified,

$$k_1 C_{O_2}(1-\theta) = \alpha k_2 C_{NH_3}\theta \tag{10}$$

where α is the number of oxygen molecules involved in the NH_3 oxidation. Classical kinetics and Eq. (10) establish the following rate expression.

$$-r = \frac{K_1 C_{o_2} K_2 C_{NH_3}}{K_1 C_{O_2} + \alpha K_2 C_{NH_3}} \tag{11}$$

Eq. (11) can be simplified as a linear function:

$$\frac{1}{-r} = \frac{\alpha}{k_1 C_{O_2}} + \frac{1}{k_2 C_{NH_3}} \tag{12}$$

The rate expression Eq. (12) refers to the oxidation NH_3 of with Cu/Ce bimetallic composite catalysts. It is determined by the Eley-Rideal (ER) kinetic expressions (Satterfield, 1991), which involve the invitation of oxygen to copper or cerium metal and the reaction of NH_3 in the gas phase with the adsorbed oxygen. When the adsorption reaction between the metal and the oxygen molecule proceeds, $k_1\ C_{O_2} >> k_2\ C_{NH_3}$ in Eq. (12), as is discussed below.

$$-r = k_2 C_{NH_3} \tag{13}$$

which refers to a first-order reaction with NH_3. This result is consistent with $\ln(1-X) = -kt$. The reaction mechanism presented herein was considered the theory to elucidate the reaction kinetics. Hence, the kinetic model was derived by assuming that a reaction proceeds between the adsorbed oxygen and the gaseous ammonia (Eley-Rideal type mechanism), by the adsorption and reduction of the ammonia onto an oxidized copper or cerium surface. Such results are consistent with those of Zawadzki (2003) and Lee (2003).

Fig. 11 compares the predicted and experimental conversions, obtained using an isothermal differential fixed-bed reactor at temperatures from 423-673 K. The figure indicates that the model accurately predicts the extent of conversion of NH_3, which increased greatly from 19.0% (423 K) to 97.0% (673 K). The removal efficiency increases with temperature and as the residence period decreases. The deviation is increased, particularly in the temperature range region 573-673 K at a high concentration of NH_3 (1000 ppm). In such a case, increasing the temperature promotes the

conversion of high concentrations of NH_3, so the extents of conversion slightly exceeded the predicted values. This model is appropriate for high concentrations of NH_3 and reactions in the presence of oxygen.

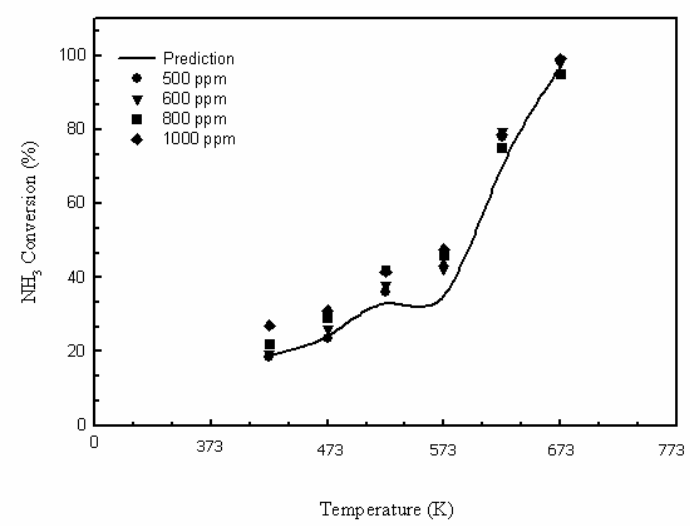

Fig. 11. Comparison of experimental data (symbols) and computed values (solid lines) from conversions of the rate equation at different temperatures and different concentrations of NH_3 by integral type model. Test conditions: 500-1,000 ppm NH_3 in He, Temp.=423-673 K, O_2=4%, R.H.=12%, GHSV=92,000 ml/h-g.

CONCLUSIONS

A composite catalyst of copper with cerium promoted the removal of ammonia by oxidation. The overall maximum selectivity of N_2 production varied from 27% to 86% and that of NO production varied from 0% to 13% over an NH_3 conversion range of 23% to 99% over a CuO-CeO_2 (6:4) bimetallic oxide catalyst. A kinetic rate expression was proposed to describe the data under the various conditions investigated. Moreover, correlation equations, in the form of Arrhenius's Law, were obtained from experimental data to specify the efficiencies of the removal of ammonia at various temperatures and residence periods in a catalytic process. The removal efficiency increases with the temperature and as the residence period is reduced. An Eley-Rideal-type kinetic model of the reaction between adsorbed oxygen and a gas-phase reactant molecule appears to represent NH_3 oxidation adequately as a first-order reaction. It is highly consistent with the experimental data. The apparent activation energy is 14.8 kcal/mol. This kinetic model is suited to reactions that involve high concentrations of NH_3 in the presence of oxygen. In this work, catalytic oxidation was found have potential for treating highly concentrated ammonia streams, helping industrial plants satisfy discharge regulations.

ACKNOWLEDGMENTS

The authors would like to thank the National Science Council of the Republic of China, Taiwan for financially supporting this research under Contract Number NSC 91-2211-E-110-003. The authors thank Professor J. C. Lou in the Institute of Environmental Engineering at National Sun Yat-Sen University for his support and discussions.

REFERENCES

Amblard, M., Burch, R. and Southward, B.W.L. (2000). A Study of the Mechanism of Selective Conversion of Ammonia to Nitrogen on Ni/γ-Al_2O_3 under Strongly Oxidizing Conditions. *Catal. Today* 59:365-371.

Auer, R. and Thyrion, F.C. (1987). Kinetics of the Total Oxidation of Methane over a $La_{0.9}Ce_{0.1}CoO_3$ Perovskite Catalyst. *Ind. Eng. Chem. Res.* 41:680-690.

Bradely, J.M., Hopkinson, A. and King, D.A. (1995). Control of a Biphasic Surface Reaction by Oxygen Coverage: the Catalytic Oxidation of Ammonia over Pt {100}. *J. Phys. Chem.* 99:17032-17042.

Burch, R. and Southward, B.W.L. (2001). The Nature of the Active Metal Surface of Catalysts for the Clean Combustion of Biogas Containing Ammonia. *J. Catal.*198:286-295.

Centi, G. and Perathoner, S. (1998). The Role of Ammonia Adspecies on the Pathways of Catalytic Transformation at Mixed Metal Oxide Surfaces. *Catal. Rev. Sci. Eng.* 40:175-208.

Chung, Y.C., Huang, C., Liu, C.H. and Bai, H. (2001). Biotreatment of Hydrogen Sulfide- and Ammonia-containing Waste Gases by Fluidized Bed Bioreactor. *J. Air & Waste. Manage. Assoc.* 51:163-172.

Curtin, T., Regan, F.O., Deconinck, C., Knűttle, N. and Hodnett, B.K. (2000). The Catalytic Oxidation of Ammonia: Influence of Water and Sulfur on Selectivity to Nitrogen over Promoted Copper Oxide/Alumina Catalysts. *Catal. Today* 55:189-195.

de Vooys, A.C.A., Koper, M.T.M., van Santen, R.A. and van Veen, J.A.R. (2001). The Role of Adsorbates in the Electrochemical Oxidation of Ammonia on Noble and Transition Metal Electrodes. *J. Electro. Chem.* 506:127-137.

Dravell, L.I., Heiskanen, K., Jones, J.M., Ross, A.B., Simell, P. and Williams, A. (2003). An Investigation of Alumina-supported Catalysts for the Selective Catalytic Oxidation of Ammonia in Biomass Gasification. *Catal. Today* 81:681-692.

Escandón, L.S., Ordóñez, S., Díez, F.V. and Sastre, H. (2002). Ammonia Oxidation over Different Commercial Oxidation Catalysts. React. *Kinet. Catal. Lett.* 76:61-67.

Fu, Q., Saltsburg, H. and Flytzani-Stephanopoulos, M. (2003). Active Nonmetallic Au and Pt Species on Ceria-based Water-gas Shift Catalysts. *Science* 301:935-938.

Gang, L., van Grondelle, J., Anderson, B.G. and van Santen, R.A. (1999). Selective Low Temperature NH_3 Oxidation to N_2 on Copper-based Catalysts. *J. Catal.* 186:100-109.

Gangwal, S.K., Mullins, M.E., Spivey, J. and Caffrey, P.R. (1988). Kinetics and Selectivity of Deep Catalytic Oxidation of n-Hexane and Benzene. *Appl. Catal.* 36:231-247.

Giroux, M., Esclassan, J., Arnaud, C. and Chalé, J.J. (1997). Analysis of Levels of Nitrates and Derivatives of Ammonia in an Urban Atmosphere. *Sci. Total. Environ.* 196:247-254.

Golunski, S.E., Hatcher, H.A., Rajaram, R.R. and Truex, T.J. (1995). Origins of Low-temperature Three-way Activity in Pt/CeO_2. *Appl. Catal. B: Environ.* 5:367-376.

González-Velasco, J.R., Gutiérrez-Ortiz, M.A., Marc, J.L., Botas, J.A., González-Marcos, M.P. and Blanchard, G.. (2003). $Pt/Ce_{0.68}Zr_{0.32}O_2$ Washcoated Monoliths for Automotive Emission Control. *Ind. Eng. Chem. Res.* 42:311-317.

Hadjiivanov, K.I. (2000). Identification of Neutral and Charged N_xO_y Surface Species by IR Spectroscopy. *Catal. Rev. Sci. Eng.* 42:71-144.

Hasegawa, T. and Sato, M. (1998). Study of Ammonia Removal from Coal-gasified Fuel. *Combust. Flame* 114:246-258.

Hashimoto, K. and Toukai, N. (2000). Decomposition of Ammonia over a Catalyst Consisting of Ruthenium Metal and Cerium Oxides Supported on Y-form Zeolite. *J. Mol. Catal. A Chem.*161:171-178.

Huang, T.L., Cliffe, K.R. and Macinnes, J.M. (2000). The Removal of Ammonia from Water by a Hydrophobic Catalyst. *Environ. Sci. Technol.* 34:4804-4809.

Hung, C.M., Lou, J.C. and Lin, C.H. (2003). Removal of Ammonia Solutions used in Catalytic Wet Oxidation Processes. *Chemosphere* 52:988-995.

Il'chenko, N.I. and Golodets, G.S. (1975a). Catalytic Oxidation of Ammonia. I. Reaction Kinetics and Mechanism. *J. Catal.* 39:57-72.

Il'chenko, N.I. and Golodets, G.S. (1975b). Catalytic Oxidation of Ammonia. II. Relationship Between Catalytic Properties of Substances and Surface Oxygen Bond Energy. General Regularities in the Catalytic Oxidation of Ammonia and Organic Substances. *J. Catal.* 39:73-86.

Il'chenko, N.I. (1976). Catalytic Oxidation of Ammonia. *Russ. Chem. Rev.* 45:1119-1134.

Kašpar, J., Fornasiero, P. and Graziani, M. (1999). Use of CeO_2-based Oxides in the Three-way Catalysis. *Catal. Today* 50:285-298.

Kim, N. J., Hirai, M. and Shoda, M. (2000). Comparison of Organic and Inorganic Packing Materials in the Removal of Ammonia Gas in Biofilters. *J. Haz. Mat.* B72:77-90.

Kurvits, T. and Marta, T. (1998). Agricultural NH_3 and NO_x Emissions in Canada. *Environ. Pollut.* 102:187-194.

Lee, J.Y., Kim, S.B. and Hong, S.C. (2003). Characterization and Reactivity of Natural Manganese ore Catalysts in the Selective Catalytic Oxidation of Ammonia to Nitrogen. *Chemosphere* 50:1115-1122.

Li, Y. and Armor, J.N. (1997). Selective NH_3 Oxidation to N_2 in a Wet Stream. *Appl. Catal. B: Environ* 13:131-139.

Liang, C., Li, W., Wei, Z., Xin, Q. and Li, C. (2000). Catalytic Decomposition of Ammonia over Nitrided MoNx/α-Al_2O_3 and NiMoNy/α-Al_2O_3 Catalysts. *Ind. Eng. Chem. Res.* 39:3694-3697.

Lietti, L., Ramis, G.., Busca, G., Bregani, F. and Forzatti, P. (2000). Characterization and Reactivity of MoO_3/SiO_2 Catalysts in the Selective Catalytic Oxidation of Ammonia to N_2. *Catal. Today* 61:187-195.

Long, R.Q. and Yang, R.T. (2001). Selective Catalytic Oxidation (SCO) of Ammonia to Nitrogen over Fe-Exchanged Zeolites. *J. Catal.* 201:145-152.

Lou, J.C. and Chen, C.L. (1995a). Destruction of Butanone and Toluene with Catalytic Incineration. *Haz. Waste & Haz. Mat.* 12:37-49.

Lou, J.C. and Lee, S.S. (1995b). Kinetics Study of Trichloromethane with Catalysis. *J. Chinese Inst. of Environ. Eng.* 5:301-307.

Lou, J.C. and Lee, S.S. (1997). Destruction of Trichloromethane with Catalytic Oxidation. *Appl. Catal. B: Environ.* 12:111-123. NOT CITED IN TEXT SEE LINE 85

Mangun, C.L., Braatz, R.D., Economy, J. and Hall, A.J. (1999). Fixed Bed Adsorption of Acetone and Ammonia onto Oxidized Activated Carbon Fibers. *Ind. Eng. Chem. Res.* 38:3499-3504.

Mojtahedi, W. and Abbasian, J. (1995). Catalytic Decomposition of Ammonia in a Fuel Gas at High Temperature and Pressure. *Fuel* 74:1698-1703.

Muenter, A. H. and Koehler, B. G. (2000). Adsorption of Ammonia on Soot at Low Temperatures. *J. Phys. Chem. A* 104:8527-8534.

Ning, W., Shen, H. and Liu, H. (2001). Study of the Effect of Preparation Method on CuO-ZnO-Al_2O_3 Catalyst. *Appl. Catal. A: General* 211:153-157.

Petryk, J. and Kolakowska, E. (2000). Cobalt Oxide Catalysts for Ammonia Oxidation Activated with Cerium and Lanthanum. *Appl. Catal. B: Environ.* 24:121-128.

Richardson, J.T. (1989). *Principles of Catalyst Development*, Plenum Press, New York.

Sadykov, V.A., Bunina, R.V., Alikina, G..M., Ivanova, A.S., Kochubei, D.I., Novgorodov, B.N., Paukshtis, E.A., Fenelonov, V.B., Zaikovskii, V.I. and Kuznetsova, T.G. (2001). Supported CuO + Ag/partially Stabilized Zirconia Catalysts for the Selective Catalytic Reduction of NO_x under Lean Burn Conditions: 1. Bulk and Surface Properties of the Catalysts. *J. Catal.* 200:117-130.

Satterfield, C.N. (1991). *Heterogeneous Catalysis in Industrial Practice*, McGraw-Hill, New York.

Schmidt-Szałowski, K., Krawczyk, K. and Petryk, J. (1998). The Properties of Cobalt Oxide Catalyst for Ammonia Oxidation. *Appl. Catal. A: General* 175:147-157.

Sedmak, G., Hočevar, S. and Levec, J. (2004). Transient Kinetic Model of CO Oxidation over a Nanostructured $Cu_{0.1}Ce_{0.9}O_{2-y}$ Catalyst. *J. Catal.* 222:87-99.

Skårman, B., Grandjean, D., Benfield, R.E., Hinz, A., Andersson, A. and Wallenberg, L.R. (2002). Carbon Monoxide Oxidation on Nanostructured CuO_x/CeO_2 Composite Particles Characterized by HREM, XPS, XAS, and High-energy Diffraction. *J. Catal.* 211:119-133.

Sotiropoulou, R.E.P., Tagaris, E. and Pilinis, C. (2004). An Estimation of the Spatial Distribution of Agricultural Ammonia Emissions in the Greater Athens Area. *Sci. Total Environ.* 318:159-169.

Spinvey, J.J. (1987). Complete Catalytic Oxidation of Volatile Organics. *Ind. Eng. Chem. Res.* 26:2165-2180.

Wang, W., Padban, N., Ye, Z., Andersson, A. and Bjerle, I. (1999). Kinetic of Ammonia Decomposition in Hot Gas Cleaning. *Ind. Eng. Chem. Res.* 38:4175-4182.

Wey, M.Y., Lu, C.Y., Tseng, H.H. and Fu, C.H. (2002). The Utilization of Catalyst Sorbent in Scrubbing Acid Gases from Incineration Flue Gas. *J. Air & Waste Manage. Assoc.* 52:449-458.

Wójtowicz, M.A., Miknis, F.P., Grimes, R.W., Smith, W.W. and Serio, M.A. (2000). Control of Nitric Oxide, Nitrous Oxide, and Ammonia Emissions Using Microwave Plasmas. *J. Haz. Mat.* 74:81-89.

Wöllner, A., Lange, F., Schmelz, H. and Knözinger, H. (1993). Characterization of Mixed Copper-manganese Oxides Supported on Titania Catalysts for Selective Oxidation of Ammonia. *Appl. Catal. A: General* 94:107-236.

Zawadzki, J. and Wiśniewski, M. (2003). In Situ Characterization of Interaction of Ammonia with Carbon Surface in Oxygen Atmosphere. *Carbon* 41:2257-2267.

Received for review, November 17, 2005
Accepted, May 1, 2006